

**OASIS**

2007  
March 26-27  
מרכז הדיזיין ת"א

The 11<sup>th</sup> Meeting on Optical Engineering and Science in Israel  
הכינוס האחד עשר לאופטיקה, אלקטרואופטיקה והנדסה אופטית

# Session 7

# Lectures:

# Control of the collapse distance in atmospheric propagation

Yonatan Sivan and Gadi Fibich

Faculty of Exact Sciences, Tel Aviv University, Tel Aviv, 69978 Israel

[yonatans@post.tau.ac.il](mailto:yonatans@post.tau.ac.il)

Yosi Ehrlich, Einat Louzon, Moshe Fraenkel

NRC Soreq, Yavneh, 81800 Israel

Shmuel Eisenmann, Yiftach Katzir, Arie Zigler

Racah Institute of Physics, Hebrew University, Jerusalem, 91904 Israel

Atmospheric propagation of high-power lasers is an active area of research, with applications such as remote sensing of the atmosphere using LIDAR applications, lightning control and military applications. Typically, Terawatt (TW) laser pulses propagate only a few meters in air before they collapse. However, various applications require control of the collapse distance  $Z_c$ .

We present a novel method to control the collapse distance based on a simple double-lens setup which consists of a defocusing and a focusing lens. The collapse distance  $Z_c^{(d)}$  is determined by varying the distance between the two lenses  $d$ . The collapse distance can be calculated by using two successive applications of the lens Transformation and is given by

$$Z_c^{(d)} = d + F_2 [Z_c (F_1 - d) - d F_1] / [(F_1 + F_2) Z_c + F_1 F_2 - d (Z_c + F_1)],$$

We observe excellent agreement between the analytical and experimental results, see Fig. 1. Our approach is superior to the standard approach for collapse control (based on negative chirping) as it 1) does not require manipulation of the pulse shape or phase, 2) enables the use of long pulses and 3) can be used to delay the collapse distance to longer distances than with negative chirping.

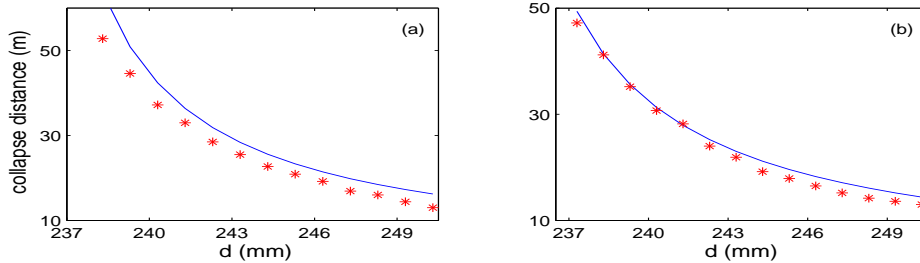


Fig. 1 Experimental (stars) and theoretical (solid line) results of the collapse distance as a function of  $d$  for powers of (a) 2 TW and (b) 3 TW.

## **Towards the Realization of Fiber Lasers in the Middle Infrared**

Irena Shafir<sup>\*</sup>, Ofer Gayer, Ariel Nause, Lev Nagli, Abraham Katzir

Raymond and Beverly Sackler Faculty of Exact Sciences, School of Physics and Astronomy, Tel-Aviv University Tel-Aviv 69978, Israel

<sup>\*</sup>Corresponding author: Tel.: +972 3 6408405; fax: +972 3 6415850; e-mail: lyakhovs@post.tau.ac.il

There is a wide interest in middle infrared lasers for countermeasures against heat seeking missiles. Most of these systems are based on diode pumped solid state lasers which pump optical parametric oscillators. These systems are bulky, expensive and hard to operate. Middle-infrared fiber lasers emitting in the 3-5.5 $\mu\text{m}$  spectral region, without need for frequency conversion, may provide an attractive alternative to these complex systems.

Although a significant effort has been made worldwide to develop such lasers, the results obtained so far have been limited, because of a lack of host materials with the desired properties such as optical transparency and low phonon energy. Silver halide crystals of the composition  $\text{AgCl}_x\text{Br}_{1-x}$  ( $0 < x < 1$ ) seem to be attractive candidates as host materials. They are highly transparent in the mid-IR, in the spectral range 3-25 $\mu\text{m}$ , they have extremely low optical phonon energies, they are non toxic and non hygroscopic and they can be extruded to form long and flexible optical fibers.

In this work we studied the optical properties of silver halide crystals and fibers doped with the following rare earth ions:  $\text{Pr}^{3+}$ ,  $\text{Nd}^{3+}$ , and  $\text{Tb}^{3+}$ . The emission, excitation, and absorption spectra, as well as the kinetic parameters, were measured. Several luminescence emission lines were found in all these crystals and fibers in the spectral range 3 - 5.5 $\mu\text{m}$ . Judd-Ofelt analysis was applied for calculation of radiative transition rates, branching ratios, and quantum efficiencies of the observed optical transitions. An attempt is being made to further improve the properties of the doped fiber, so that fiber lasers could be made.

According to this analysis it seems that the rare earth doped  $\text{AgClBr}$  crystals would be useful for the fabrication of solid state lasers and fiber lasers for the spectral range 3 - 5.5 $\mu\text{m}$ . These would be extremely useful for counter measures which will protect civilian airplanes against terrorist attacks.

# **HIGH-POWER LASERS IN DEFENSE AND SECURITY**

Yehoshua Socol

Yosef Pinhasi

Dept. of Electrical and Electronic Engineering. The College of Judea and Samaria, Ariel  
socol@yosh.ac.il

Laser-based ("directed energy") defense and security projects are on rise, with NAUTILUS anti-missile project as a recent well-known example. The presentation will give an outline of available public-domain data on different past and present high-power-laser projects (including Soviet experience with CO<sub>2</sub> lasers), analyzing goals and basic technologies. Ballistic, beam-riding and self-guiding missiles' counter-measures (based on laser technologies) will be discussed. Achievements, advantages and drawbacks of Free Electron Laser, CO<sub>2</sub> and other high-power laser technologies will be briefly reviewed.

# **SPECTRAL MULTIPLEXING APPROACH**

## **FOR HYPERSPECTRAL CAMERA-ON-CHIP**

Michael A. Golub<sup>1</sup>, Menachem Nathan<sup>1</sup>, Amir Averbuch<sup>2</sup> and Alon Schclar<sup>2</sup>

<sup>1</sup> - Department of Physical Electronics, Faculty of Engineering, <sup>2</sup> - School of Computer Science, Faculty of Exact Sciences, Tel Aviv University, Ramat Aviv, 69978, Israel,  
e-mail: mgolub@eng.tau.ac.il.

Spectral (including hyperspectral) imaging provides a 2-D image of a polychromatic object in several parts of the spectrum. There are many known and potential uses of such imaging in biology, chemistry and remote sensing. Spectral imaging combines imaging and spectral analysis in a single device. The problem can be stated as how to access 3-D (spatial and spectral) data by a 2-D photodetector array and dispersive optical element.

Our method involves introduction of an intentional image pixel spread and of a small lateral dispersive shift of the spectral components of each image pixel by a weak dispersive element (weakly diffracting diffraction grating or prism). Therefore, spectral components of different image pixels in a 2-D image related to different points of the object are shifted and overlapped, i.e. there is "spectral multiplexing". The intensity of the multiplexed image is read by a monochrome imager chip (e.g. CCD or CMOS type) and processed by an algorithm of digital spectral restoration or "de-multiplexing", for the subsequent digital restoration of the image at each wavelength band of the spectrum. Relations between image feature size, full spectral range and number of spectral bands are discussed. A match required between the actual image and the dispersive shift is an important feature of our method. In particular, the complete lateral dispersive shift needs to be equal to the image feature size. The restoration (de-multiplexing) reflects a "compromise" between spatial and spectral resolutions of the image.

Results of computer simulations show that our method enables a regular digital imaging system based on an imager "chip" (e.g. CCD or CMOS type) and equipped with a light dispersing element to serve as an imaging spectrometer and to perform as a hyperspectral camera on chip. In other words, our method allows the instantaneous acquisition of an entire image or data "cube", i.e. the instantaneous acquisition of all three dimensions (two spatial and one spectral) of the image. This is in contrast with all known spectral imaging methods that allow only acquisition of two-dimensional image data (i.e. two of the three dimensions) at a time.

# **DETECTION OF GASEOUS PLUME IN IR HYPERSPECTRAL IMAGES USING SPATIAL MODIFIED K-MEANS**

Eitan Hirsch<sup>a</sup> Eyal Agassi<sup>b</sup>,

<sup>a</sup>Life Science Research Israel

<sup>b</sup>Israel Institute for Biology Research;

P.O. Box 19, Nes Ziona, 74100 Israel

[hirsch-eitan@iibr.gov.il](mailto:hirsch-eitan@iibr.gov.il)

The emergence of IR hyperspectral sensors in the last recent years enables their employment for remote environmental monitoring of gaseous plumes. IR hyperspectral imaging combines the unique advantages of the traditional remote sensing methods such as multispectral imagery and non-imaging FTIR, while eliminating their drawbacks. The most significant upgrade introduced by hyperspectral technology in the capabilities of standoff detection and discrimination of effluent gaseous plumes without a clear reference background, or any other temporal information. In this paper, we introduce a novel approach aimed to detect and discriminate gaseous plumes in IR hyperspectral imagery using spatial-spectral K-means segmentation. The utility of the suggested detection algorithm is demonstrated on acquired IR hyperspectral images of two atmospheric traces released into a free atmosphere. Applying the proposed detection method over the experimental data has yielded a correct classification in all the releases without any misclassification. These encouraging results show that the presented approach can be used as a core of complete classification algorithm for gaseous pollutants plumes in IR hyperspectral imagery without a need for a clean background.

## **Turbulent video enhancement: Image stabilization and super-resolution**

**Barak Fishbain**, Ianir Idess, Shai Gepstein, Leonid Yaroslavsky  
Tel-Aviv University, Tel Aviv 69978, Israel Phone: 972-3-640-8014 Fax: 972-3-641-0189.  
ianir}@eng.tau.ac.ilmail: {barak | yaro |

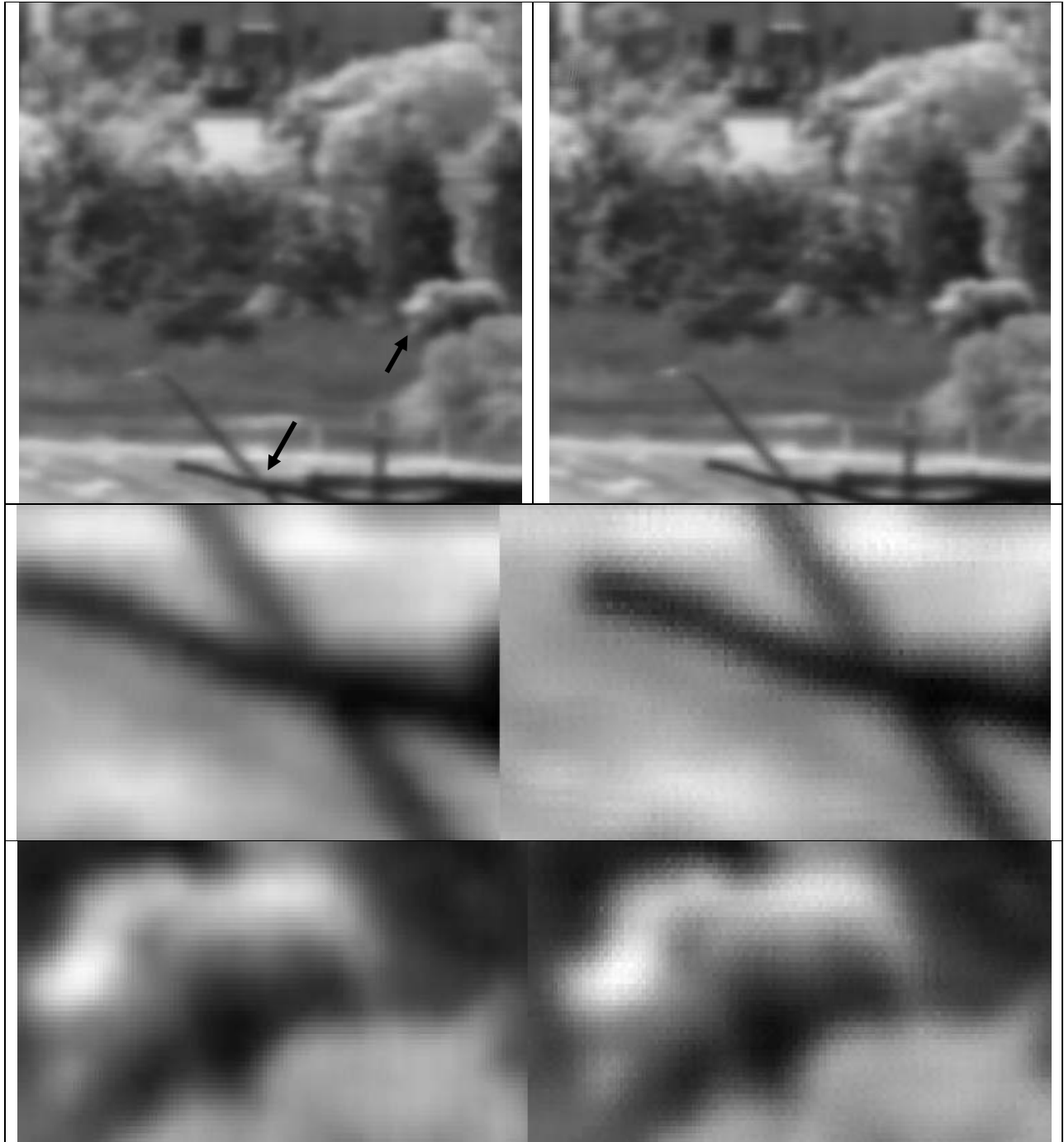
Image and video quality in Long Range Observation Systems (LOROS) suffer from atmospheric turbulence that causes small neighbourhoods in image frames to randomly move in different directions and substantially hampers visual analysis of such video sequences. Images are also blurred both by atmospheric turbulence, and camera optics and image sampling. The paper presents a set of methods to substantially enhance image visual quality through image stabilization and resolution enhancement.

Image stabilization is achieved through the following three steps of video processing: (i) estimation of the steady scene, (ii) real motion extraction, and (iii) generation of stabilized and resolution enhanced frames. For estimation of the stable scene from a sequence of turbulent frames, a pixel-wise rank-order filtering in a temporal window implemented through fast recursive algorithms is used. For extraction of real moving objects in the scene, pixel-wise motion vectors are computed for each frame and statistical cluster analysis of motion vector amplitude and direction is used to separate motions caused by atmospheric turbulence from those of real moving objects. Stabilized frames are generated as a combination of the steady scene estimation in those pixels where no real motion is detected and of pixels belonging to corresponding moving objects wherever such a motion was detected. The motion vector maps for all frames are also used to enhance the resolution of the stabilized frames. This is achieved by replacement of pixels in an interpolated estimation of the steady scene by pixels from the frames according to their position defined by their motion vector. The super-resolved image is a better candidate than the original one for image processing tools such as aperture correction and noise filtering. This means that applying digital image processing techniques on the super-resolved images improves the visual quality more than applying the same techniques on the original frame.

As experiments show, such stabilized and “super-resolved” video sequences generated from real-life observation systems video sequences demonstrate substantial improvement in image resolution and quality. Examples of stabilized video can be found in [http://www.eng.tau.ac.il/~yaro/ShaiGepshtein/movie\\_no\\_turb.zip](http://www.eng.tau.ac.il/~yaro/ShaiGepshtein/movie_no_turb.zip). Super resolution from turbulent motion is illustrated in the figure. The stabilized frame extracted from real-life turbulent sequence is presented beside to the same frame after super-resolution applied. To allow better analysis, two fragments of both frames are presented as well. For all figures, the left hand side presents the fragments in their original resolution, while the right-hand side shows the same fragments after applying super-resolution.

**KEYWORDS:**

**LOROS, Super-Resolution, Turbulence-Compensation, Real-Time, Rank-Filtering, Optical-Flow**



*Super Resolution from Turbulent Motion. The left-hand side is the stabilized image extracted from a real life sequence. The right-hand frame is the same frame with super-resolution applied.*